JACS
JOURNAL OF THE AMERICAN CHEMICAL SOCIETY

COMMUNICATION

pubs.acs.org/JACS

Development of an Si-Rhodamine-Based Far-Red to Near-Infrared Fluorescence Probe Selective for Hypochlorous Acid and Its Applications for Biological Imaging

Yuichiro Koide,[†,‡] Yasuteru Urano,[§] Kenjiro Hanaoka,[†,‡] Takuya Terai,[†,‡] and Tetsuo Nagano*[,†,‡]

[†]Graduate School of Pharmaceutical Sciences and [§]Graduate School of Medicine, The University of Tokyo, Hongo, Bunkyo-ku, Tokyo 113-0033, Japan

[‡]CREST, JST, Japan Science and Technology Agency, 3-5 Sanbancho, Chiyoda, Tokyo 102-0075, Japan

S *Supporting Information* *W* *Web-Enhanced*

ABSTRACT: A far-red to near-infrared (NIR) fluorescence probe, MMSiR, based on Si-rhodamine, was designed and synthesized for sensitive and selective detection of HOCl in real time. MMSiR and its oxidized product SMSiR have excellent properties, including pH-independence of fluorescence, high resistance to autoxidation and photobleaching, and good tissue penetration of far-red to NIR fluorescence emission. The value of MMSiR was confirmed by real-time imaging of phagocytosis using a fluorescence microscope. wsMMSiR, a more hydrophilic derivative of MMSiR, permitted effective in vivo imaging of HOCl generation in a mouse peritonitis model. This probe is expected to be a useful tool for investigating the wide range of biological functions of HOCl.

Reactive oxygen species (ROS) and reactive nitrogen species (RNS) mediate a wide variety of biological events.[1] Among the ROS, hypochlorous acid (HOCl), which is produced mainly in leukocytes (including neutrophils, macrophages, and monocytes) by myeloperoxidase (MPO)-catalyzed peroxidation of chloride ions,[2] is centrally linked to innate host defense, playing a vital role in killing a wide range of pathogens.[3] On the other hand, oxidative stress due to excessive generation of ROS is implicated in many human diseases,[4] and it is considered that neutrophil-derived HOCl contributes to inflammation-associated tissue injury, such as hepatic ischemia-reperfusion injury,[5] atherosclerosis,[6] lung injury,[7] and rheumatoid arthritis.[8] Nevertheless, the biological activities of HOCl have not yet been fully established. A number of methods for detection of HOCl have been developed.[9−13] Among them, fluorescence imaging methods are generally superior in terms of sensitivity, spatial and temporal resolution, and ease of use. Although several HOCl probes have been developed,[14−18] only a few meet the requirements of (1) high sensitivity and selectivity for HOCl, (2) high resistance to autoxidation and photobleaching, and (3) suitability for biological applications in vitro and in vivo.

Our group has reported a HOCl-selective probe based on rhodamine, HySOx (Figure 1).[19] HySOx shows high and specific signal amplification in response to HOCl, and the fluorescent product formed after reaction with HOCl has favorable characteristics for biological imaging, including high water solubility,

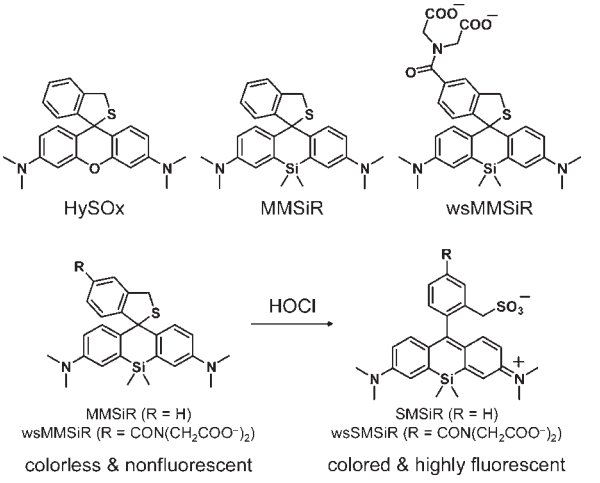

Figure 1. Structures and design of HySOx and newly developed far-red to NIR-emitting fluorescence probes for HOCl.

high fluorescence intensity, pH-independent fluorescence, and tolerance to photobleaching. In short, HySOx is an excellent HOCl probe with absorption and emission maxima in the visible region. However, it is well established that probes operating in the far-red to near-infrared (NIR) region have many advantages for biological applications, including low phototoxicity, low autofluorescence, and good tissue penetration.[20] Therefore, we examined whether the HOCl detection mechanism used in HySOx, i.e., release from the spiro-cyclized form by oxidation of the S atom, would also be applicable to Si-rhodamine,[21,22] which has its absorption and emission maxima at around 650 nm, while retaining the other excellent characteristics of rhodamine. For this purpose, we designed and synthesized MMSiR (Figure 1) as a novel far-red to NIR-emitting HOCl-sensitive fluorescence probe, by reacting a lithiated benzene moiety bearing a mercaptomethyl group protected by *tert*-butyl group with Si-xanthone (see Scheme S1 in the Supporting Information (SI)), and the overall yield of MMSiR was 46%. We then confirmed that MMSiR emits in the far-red to NIR region after reaction with HOCl. Further, in a preliminary experiment to confirm the superior imaging potential of our far-red to NIR-emitting probe, we found that relative fluorescence detected at the

Received: December 21, 2010
Published: March 28, 2011

dx.doi.org/10.1021/ja111470n | *J. Am. Chem. Soc.* 2011, 133, 5680–5682

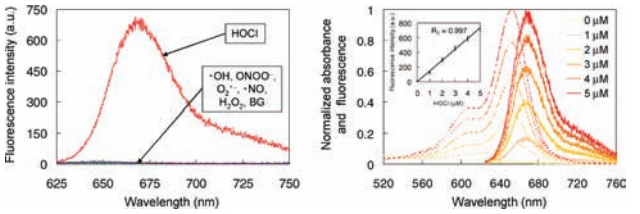

Figure 2. (Left) Fluorescence spectra of 5 μM MMSiR before and after reaction with various ROS in PBS at pH 7.4, containing 0.1% DMF. HOCl = NaOCl (final 5 μM) was added and the mixture was stirred at 37 °C. $^{\bullet}$OH = ferrous perchlorate (500 μM) and H_2O_2 (1 mM) were added at room temperature. $ONOO^-$ = $ONOO^-$ (final 5 μM) was added and the mixture was stirred at 37 °C. $O_2^{-\bullet}$ = KO_2 (100 μM) was added and the mixture was stirred at 37 °C for 30 min. H_2O_2 = H_2O_2 (100 μM) was added and the mixture was stirred at 37 °C for 30 min. $^{\bullet}$NO = NOC7 (5 μM) was added and the mixture was stirred at 37 °C for 30 min. BG = background. Excitation wavelength was 620 nm. (Right) Absorbance and fluorescence spectra of MMSiR before and after reaction with HOCl (0 to 5 μM). Inset shows a linear response of fluorescence to the concentration of HOCl.

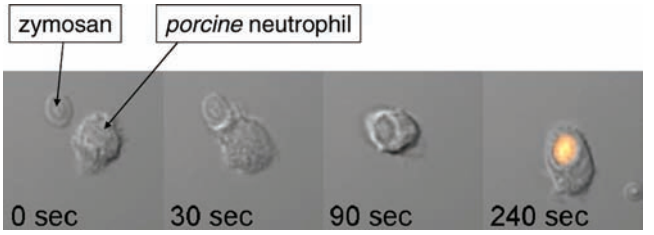

Figure 3. Fluoresence microscopic imaging of phagocytosis of opsonized zymosan by 1 μM MMSiR-loaded porcine neutrophil. Opsonized zymosan particle is located near the neutrophil (0 s). The neutrophil engulfs the zymosan (30 s). Phagosytosis is complete (90 s). HOCl generated in the phagosome was detected with MMSiR (240 s).

Ⓦ A video of this imaging is available.

abdomen of mice after intraperitoneal administration was 1 order of magnitude greater with the Si-rhodamine than with the visible light-emitting O-rhodamine (Figure S1, SI), which clearly indicates the superiority of MMSiR over HySOx for in vivo use.

Next, we examined the sensitivity and selectivity of MMSiR for HOCl over other ROS (Figure 2). Although MMSiR was scarcely fluorescent before detection of HOCl, when it reacted with HOCl, a large and immediate increase of fluorescence intensity was observed, owing to the formation of highly fluorescent SMSiR (Abs_{max}/Em_{max} = 652/670 nm, $\varepsilon = 1.2 \times 10^5$, $\Phi_{fl} = 0.31$, in PBS), and the fluorescence intensity change was linearly related to the concentration of HOCl. In contrast, other ROS ($^{\bullet}$OH, $ONOO^-$, $O_2^{-\bullet}$, $^{\bullet}$NO, H_2O_2) produced almost no fluorescence increase. Thus, MMSiR appears to be highly sensitive and selective for the detection of HOCl. In addition, we examined the fluorescence response of MMSiR in the presence of a HOCl-generating enzymatic system (Figure S3, SI). The fluorescence was increased, and the increase was suppressed by a MPO inhibitor. Furthermore, we confirmed the photostability of SMSiR and the pH-independence of its fluorescence (Figures S4 and S5, SI). Thus, MMSiR can sensitively and selectively detect HOCl in real time, and its oxidized product, SMSiR, has excellent properties as a fluorophore.

With these results in hand, we first applied MMSiR to image the generation of HOCl during phagocytosis by porcine neutrophils,[19,23] using a confocal microscope with the widely employed 633 nm excitation laser and Cy5 filter set. When opsonized zymosan derived

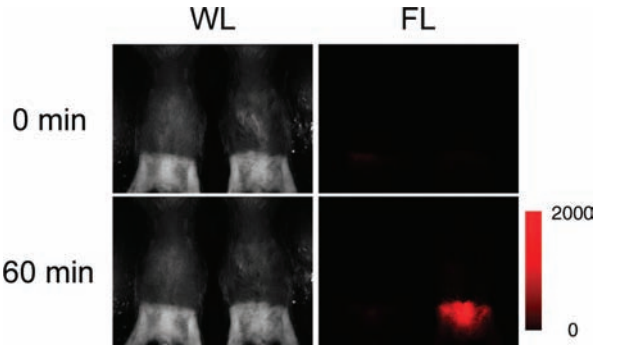

Figure 4. Comparison of white light (WL) and 750 nm fluorescence (FL) images of unstimulated mouse (left) and the peritonitis model mouse stimulated with zymosan and PMA (right). 50 μM wsMMSiR in 0.8 mL of saline and 0.3 μg of PMA in 0.3 mL saline were successively administered by intraperitoneal injection. Images were obtained just before (0 min) and 60 min after PMA injection. Representative data are shown (n = 3).

from *Saccharomyces cerevisiae* was added to MMSiR-loaded porcine neutrophils, we observed that neutrophils engulfed zymosan particles, followed by enhancement of the fluorescence signal inside the phagosomes (Figure 3 and supporting movie). During the imaging of phagocytosis, little fluorescence increase due to excitation laser-induced autoxidation could be seen, and there was no observed decrease of the fluorescence signal due to photobleaching after completion of phagocytosis. Thus, MMSiR is extremely effective for detecting HOCl generation during phagocytosis and should be suitable for practical use in vitro.

We next assessed the ability of our probe to visualize HOCl in a mouse peritonitis model. To obtain a sufficiently high concentration for efficient in vivo imaging, we prepared the more hydrophilic derivative wsMMSiR, bearing hydrophilic dicarboxylic acid structure. C57BL/6 mice were given an i.p. injection of zymosan to induce neutrophils to invade the peritoneal cavity.[24,25] After 4 h, the mice were anesthetized, and the abdominal fur was removed. Then, the mice were injected i.p. with wsMMSiR, and 5 min later, PMA was i.p. injected. The fluorescence measured at the abdomen increased markedly after PMA injection, and strong fluorescence was observed at 60 min (Figure 4). In contrast, control, unstimulated mice that were i.p. injected with the probe followed by saline only (no zymosan or PMA) showed no significant fluorescence enhancement. Thus, our far-red to NIR probe is applicable for not only in vitro imaging but also in vivo imaging.

In summary, we have designed and synthesized a novel far-red to NIR fluorescence probe, MMSiR, based on Si-rhodamine. MMSiR can sensitively and selectively detect HOCl in real time, and MMSiR and its oxidized product SMSiR have excellent properties for biological applications, including pH-independence and tolerance to autoxidation and photobleaching during excitation laser irradiation. With MMSiR, we conducted real-time imaging of phagocytosis by means of fluorescence microscopy, and, with the more hydrophilic derivative wsMMSiR, we achieved noninvasive in vivo imaging of HOCl generation in a mouse peritonitis model. Our probe is expected to be a useful tool for investigation of the wide range of biological functions of HOCl.

■ ASSOCIATED CONTENT

Ⓢ **Supporting Information.** Synthesis; experimental details; characterization of MMSiR, SMSiR, and wsMMSiR; and

experiments using living cells and mice. This material is available free of charge via the Internet at http://pubs.acs.org.

Web Enhanced Feature. A video in .avi format is available in the HTML version of this Communication, showing the fluoresence microscopic imaging of phagocytosis of opsonized zymosan by 1 μM MMSiR-loaded porcine neutrophil.

AUTHOR INFORMATION

Corresponding Author
tlong@mol.f.u-tokyo.ac.jp

ACKNOWLEDGMENT

This research was supported in part by a Grant-in-Aid for Scientific Research (Specially Promoted Research 22000006 to T.N., and Grant Nos. 20117003 and 19205021 to Y.U.) by the Ministry of Education, Culture, Sports, Science and Technology of Japan.

REFERENCES

(1) Lambeth, J. D. *Free. Radic. Biol. Med.* **2007**, *43*, 332–347.
(2) Pattison, D. I.; Davies, M. J. *Biochemistry* **2006**, *45*, 8152–8162.
(3) Prokopowicz, Z. M.; Arce, F.; Biedroń, R.; Chiang, C. L.; Ciszek, M.; Katz, D. R.; Nowakowska, M.; Zapotoczny, S.; Marcinkiewicz, J.; Chain, B. M. *J. Immunol.* **2010**, *184*, 824–835.
(4) Roberts, R. A.; Laskin, D. L.; Smith, C. V.; Robertson, F. M.; Allen, E. M.; Doorn, J. A.; Slikker, W. *Toxicol. Sci.* **2009**, *112*, 4–16.
(5) Hasegawa, T.; Malle, E.; Farhood, A.; Jaeschke, H. *Am. J. Physiol. Gastrointest. Liver Physiol.* **2005**, *289*, 760–767.
(6) Daugherty, A.; Dunn, J. L.; Rateri, D. L.; Heinecke, J. W. *J. Clin. Invest.* **1994**, *94*, 437–444.
(7) Hammerschmidt, S.; Büchler, N.; Wahn, H. *Chest* **2002**, *121*, 573–581.
(8) Wu, S. M.; Pizzo, S. V. *Arch. Biochem. Biophys.* **2001**, *391*, 119–126.
(9) March, J. G.; Gual, M.; Simonet, B. M. *Talanta* **2002**, *58*, 995–1001.
(10) Moberg, L.; Karlberg, B. *Anal. Chim. Acta* **2000**, *207*, 127–133.
(11) Ballesta Claver, J.; Valencia Mirón, M. C.; Capitán-Vallvey, L. F. *Anal. Chim. Acta* **2004**, *522*, 267–273.
(12) Setsukinai, K.; Urano, Y.; Kakinuma, K.; Majima, H. J.; Nagano, T. *J. Biol. Chem.* **2003**, *278*, 3170–3175.
(13) Koide, Y.; Urano, Y.; Kenmoku, S.; Kojima, H.; Nagano, T. *J. Am. Chem. Soc.* **2007**, *129*, 10324–10325.
(14) Chen, S.; Lu, J.; Sun, C.; Ma, H. *Analyst* **2010**, *135*, 577–582.
(15) Panizzi, P.; Nahrendorf, M.; Wildgruber, M.; Waterman, P.; Figueiredo, J. L.; Aikawa, E.; McCarthy, J.; Weissleder, R.; Hilderbrand, S. A. *J. Am. Chem. Soc.* **2009**, *131*, 15739–15744.
(16) Sun, Z.; Liu, F.; Chen, Y.; Tam, P. K. H.; Yang, D. *J. Org. Chem.* **2008**, *10*, 2171–2174.
(17) Lin, W.; Long, L.; Chen, B.; Tan, W. *Chem. Eur. J.* **2009**, *15*, 2305–2309.
(18) Shepherd, J.; Hilderbrand, S. A.; Waterman, P.; Heinecke, J. W.; Weissleder, R.; Libby, P. *Chem. Biol.* **2007**, *14*, 1221–1231.
(19) Kenmoku, S.; Urano, Y.; Kojima, H.; Nagano, T. *J. Am. Chem. Soc.* **2007**, *129*, 7313–7318.
(20) Weissleder, R. *Nat. Biotechnol.* **2001**, *19*, 316–317.
(21) Koide, Y.; Urano, Y.; Hanaoka, K.; Terai, T.; Nagano, T. *ACS Chem. Biol.* **2011**No. DOI: 10.1021/cb1002416.
(22) Fu, M.; Xiao, Y.; Qian, X.; Zhao, D.; Xu, Y. *Chem. Commun.* **2008**, *15*, 1780–1782.
(23) Dickinson, B. C.; Huynh, C.; Chang, C. J. *J. Am. Chem. Soc.* **2010**, *132*, 5906–5915.
(24) Haribabu, B.; Verghese, M. W.; Steeber, D. A.; Sellars, D. D.; Bock, C. B.; Snyderman, R. *J. Exp. Med.* **2000**, *192*, 433–438.
(25) Frasch, S. C.; Berry, K. Z.; Fernandez-Boyanapalli, R.; Jin, H. S.; Leslie, C.; Henson, P. M.; Murphy, R. C.; Bratton, D. L. *J. Biol. Chem.* **2008**, *283*, 33736–33749.